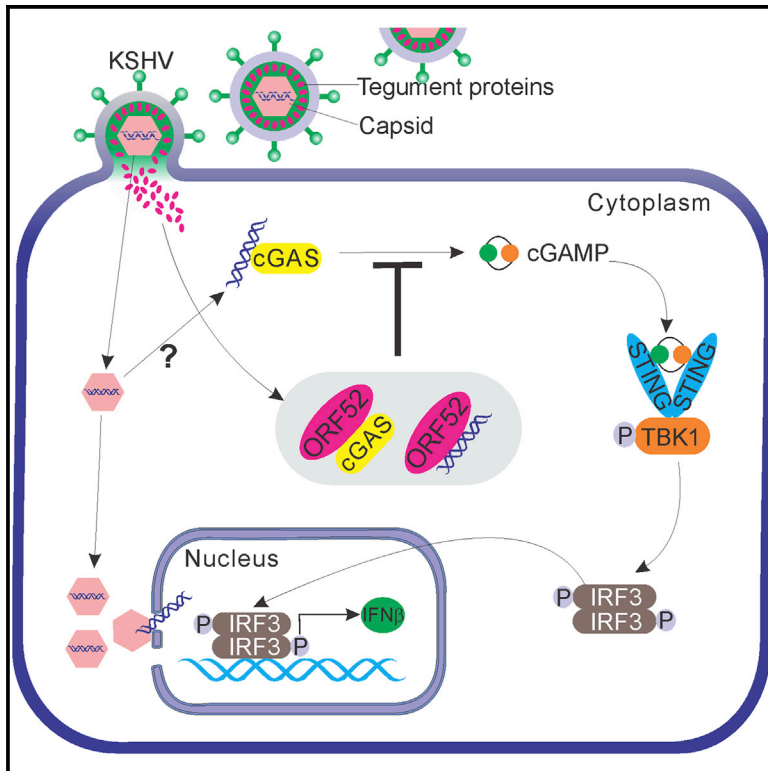


# Cell Host & Microbe

## Inhibition of cGAS DNA Sensing by a Herpesvirus Virion Protein

### Graphical Abstract



### Authors

Jian-jun Wu, Wenwei Li, Yaming Shao, ..., Denise Whitby, Hong Li, Fanxiu Zhu

### Correspondence

fzhu@bio.fsu.edu

### In Brief

cGAS is the principal cytosolic DNA sensor that detects invading viral DNA and triggers antiviral responses. Wu et al. reveal that a gammaherpesvirus-conserved protein, ORF52, binds to DNA and cGAS and directly inhibits cGAS enzymatic activity, thereby antagonizing host cGAS-dependent DNA sensing.

### Highlights

- KSHV ORF52 prevents cGAS DNA sensing by directly inhibiting cGAS enzymatic activity
- The inhibition of cGAS by ORF52 requires binding to both DNA and cGAS
- The inhibition of cGAS by ORF52 is conserved among gammaherpesviruses
- KSHV can elicit cGAS-dependent immune responses that are counteracted by ORF52



# Inhibition of cGAS DNA Sensing by a Herpesvirus Virion Protein

Jian-jun Wu,<sup>1,7</sup> Wenwei Li,<sup>1,7</sup> Yaming Shao,<sup>2</sup> Denis Avey,<sup>1</sup> Bishi Fu,<sup>1</sup> Joseph Gillen,<sup>1</sup> Travis Hand,<sup>2</sup> Siming Ma,<sup>1</sup> Xia Liu,<sup>1</sup> Wendell Miley,<sup>4</sup> Andreas Konrad,<sup>5</sup> Frank Neipel,<sup>6</sup> Michael Stürzl,<sup>5</sup> Denise Whitby,<sup>4</sup> Hong Li,<sup>2,3</sup> and Fanxiu Zhu<sup>1,\*</sup>

<sup>1</sup>Department of Biological Science, Florida State University, Tallahassee, FL 32306, USA

<sup>2</sup>Institute of Molecular Biophysics

<sup>3</sup>Department of Chemistry and Biochemistry

Florida State University, Tallahassee, FL 32306, USA

<sup>4</sup>Viral Oncology Section, AIDS and Cancer Virus Program, Frederick National Laboratory for Cancer Research, Frederick, MD 21702, USA

<sup>5</sup>Division of Molecular and Experimental Surgery, Department of Surgery, University Medical Center Erlangen, Friedrich-Alexander-University Erlangen-Nürnberg, Erlangen 91054, Germany

<sup>6</sup>Institute of Clinical and Molecular Virology, University of Erlangen-Nürnberg, Schlossgarten 4, D-91054 Erlangen, Germany

<sup>7</sup>Co-first author

\*Correspondence: [fzhu@bio.fsu.edu](mailto:fzhu@bio.fsu.edu)

<http://dx.doi.org/10.1016/j.chom.2015.07.015>

## SUMMARY

Invading viral DNA can be recognized by the host cytosolic DNA sensor, cyclic GMP-AMP (cGAMP) synthase (cGAS), resulting in production of the second messenger cGAMP, which directs the adaptor protein STING to stimulate production of type I interferons (IFNs). Although several DNA viruses are sensed by cGAS, viral strategies targeting cGAS are virtually unknown. We report here that Kaposi's sarcoma-associated herpesvirus (KSHV) ORF52, an abundant gammaherpesvirus-specific tegument protein, subverts cytosolic DNA sensing by directly inhibiting cGAS enzymatic activity through a mechanism involving both cGAS binding and DNA binding. Moreover, ORF52 homologs in other gammaherpesviruses also inhibit cGAS activity and similarly bind cGAS and DNA, suggesting conserved inhibitory mechanisms. Furthermore, KSHV infection evokes cGAS-dependent responses that can limit the infection, and an ORF52 null mutant exhibits increased cGAS signaling. Our findings reveal a mechanism through which gammaherpesviruses antagonize host cGAS DNA sensing.

## INTRODUCTION

Cytosolic DNA derived from microbial pathogens represents a potent pathogen-associated molecular pattern (PAMP) that triggers the host innate immune responses by stimulating production of type I interferons (IFNs). The cyclic guanosine monophosphate-adenosine monophosphate (cGAMP) synthase (cGAS) has recently been identified as the principal sensor of cytosolic DNA (Cai et al., 2014; Sun et al., 2013; Wu et al., 2013). Binding of DNA to cGAS activates its enzymatic activity, producing cGAMP from ATP and GTP (Cai et al., 2014; Civril et al., 2013; Gao et al., 2013b; Kranzusch et al., 2013; Li et al.,

2013a; Zhang et al., 2014). As a second messenger, cGAMP binds to and activates the stimulator of interferon genes (STING) in infected cells, as well as neighboring cells, through cell-cell junctions (Ablasser et al., 2013a, 2013b; Gao et al., 2013c). Active STING then activates TANK-binding kinase 1 (TBK1) to phosphorylate and activate interferon regulatory factor 3 (IRF3), ultimately leading to expression of type I IFNs (Barber, 2014; Tanaka and Chen, 2012). DNA viruses, including herpes simplex virus 1 (HSV-1), vaccinia virus, and adenovirus, as well as retroviruses, such as HIV-1, have been shown to be sensed by cGAS (Dai et al., 2014; Gao et al., 2013a; Lam et al., 2014; Li et al., 2013b). Because activation of cGAS elicits a potent antiviral response (Li et al., 2013b; Schoggins et al., 2014), viruses must possess mechanisms to subvert the cGAS-cGAMP signaling pathway to establish successful infection. To date, no such mechanisms have been described.

Kaposi's sarcoma-associated herpesvirus (KSHV) is the causative agent of Kaposi's sarcoma (KS), primary effusion lymphoma, and a subset of multicentric Castlemann's disease (Cesarman et al., 1995; Chang et al., 1994; Ganem, 2007; Soulier et al., 1995). Like other herpesviruses, KSHV exhibits two alternative life cycles: latent and lytic. KSHV primarily establishes latency, during which only a handful of genes are expressed and no progeny are produced. Lytic replication constitutes expression of the full complement of viral genes in a temporal cascade, ultimately resulting in the production of progeny virions (Ganem, 2007). A low level of spontaneous lytic reactivation occurs in the lesions of KSHV-associated diseases, and is believed to be required for viral persistence and pathogenesis (Ganem, 2010). Although the capsid-enclosed herpesviral DNA is believed to be delivered into the nucleus, where herpesviruses replicate their genomes, viral DNA could leak into the cytosol and subsequently be sensed by cGAS (Horan et al., 2013; Paludan et al., 2011). It is thus possible that KSHV infection could elicit cGAS-dependent responses and that the virus possesses a mechanism(s) to subvert cGAS-cGAMP signaling in order to evade the innate immune response. However, no viral strategies that target cGAS have been described. We report here that KSHV ORF52, a gammaherpesvirus-specific tegument protein, inhibited cGAS enzymatic activity via a mechanism involving its

binding to DNA and cGAS. Furthermore, ORF52 homologs in other gammaherpesviruses also inhibited cGAS. Moreover, we found that KSHV primary infection elicits cGAS- and STING-dependent responses that can be partially mitigated by ORF52. Our results reveal KSHV ORF52 as an inhibitor of cGAS, and we propose to name it KSHV inhibitor of cGAS, KicGAS.

## RESULTS

### KSHV ORF52 Inhibits cGAS DNA-Sensing Signaling

We reasoned that a potential cGAS inhibitor would be a virion component, localize to the cytoplasm, and interact with DNA and/or cGAS. Systematic analysis of all KSHV proteins for inhibition of cGAS-dependent IFN $\beta$  production revealed eight viral protein candidates as cGAS signaling antagonists (see Figure S1A available online). Among them, ORF52 was the only protein confirmed to bind to DNA (Figures S1B and S1C). ORF52 was previously shown to be an abundant virion protein (Zhu et al., 2005) and localize exclusively to the cytoplasm (Sander et al., 2008), making it a prime candidate for an inhibitor of cGAS. To determine whether ORF52 has an effect on the cGAS signaling pathway, we coexpressed cGAS with IFN $\beta$  luciferase reporter in the presence or absence of ORF52 in HEK293T cells stably expressing STING (HEK293T/STING). Transfection of cGAS increased IFN $\beta$  promoter-driven luciferase activity by more than 150-fold, but coexpression with ORF52 reduced cGAS-induced luciferase activity by more than 80% (Figure 1A). The inhibition appeared to be specific to cGAS, because ORF52 had little effect on luciferase activity induced by the cytosolic RNA sensor RIG-I (Figure 1A). In agreement with the inhibition of luciferase reporter activity, cGAS-mediated dimerization and phosphorylation of IRF3 were inhibited by ORF52 (Figure 1B) in a dose-dependent manner (Figure S2A). Furthermore, while HEK293T/STING cells expressing cGAS displayed a strong antiviral effect to vesicular stomatitis virus (VSV-GFP) infection (14.7% infection), coexpression with ORF52 partially relieved this effect (53.5% infection), suggesting that ORF52 specifically inhibits cGAS-dependent antiviral responses (Figure 1C).

The human monocyte cell line THP-1 expresses most cytosolic DNA sensors and has been used extensively for their study (Sun et al., 2013; Wu et al., 2013; Zhang et al., 2011). We made use of the reporter cell line THP1 Lucia ISG (Invivogen), which expresses luciferase from a gene under the control of an IRF3-inducible ISG54 promoter, as a surrogate assay to measure induction of the innate immune response by nucleic acid sensors. We transduced these cells with a lentiviral vector expressing ORF52 from a doxycycline-inducible promoter or with control empty vector (pEasiLV). We found that expression of ORF52 reduced luciferase activity induced by interferon stimulatory DNA 45-mer (ISD45), but not by RNA Poly(I:C) (Figure 1D). ORF52 expression also reduced the dimerization and phosphorylation of IRF3, confirming its specific inhibition of DNA- but not RNA-induced activation of IRF3 (Figure 1E). Similarly, ORF52 also reduced luciferase activity induced by the DNA virus vaccinia (VACV), but not by the RNA virus Sendai (SEV) (Figure 1F), in a dose-dependent manner (Figure S2B). Furthermore, purified ORF52 protein directly transfected after fusion with TAT cell-penetrating peptide (Figures S2C–S2E) also inhibited

DNA- but not RNA-dependent responses, further confirming our previous results (Figures 1G–1I). Together, these data suggest that KSHV ORF52 selectively inhibits cGAS DNA-sensing signaling.

### ORF52 Inhibits cGAS Enzymatic Activity

Although ORF52 inhibited DNA- and cGAS-triggered dimerization and phosphorylation of IRF3, it had no apparent effect on cGAMP-induced activation of IRF3 (Figures 2A and 2B), suggesting that ORF52 inhibits cGAS directly. Because cGAS catalyzes synthesis of cGAMP upon binding to DNA, we examined the effect of ORF52 protein on cGAS enzymatic activity. We expressed human cGAS (hcGAS) and ORF52 in bacteria and purified them to homogeneity (Figure 2C). The purified hcGAS catalyzed the production of cGAMP only when ISD45 was included in the reaction. Approximately 70% of [ $\alpha$ - $^{32}$ P]-ATP was converted to cGAMP in 2 hr under our assay conditions (Figure 2D). Inclusion of ORF52 in the reaction reduced production of cGAMP in a dose-dependent manner, from 40% at an ORF52:cGAS molar ratio of 1:1 to complete inhibition at a ratio of 4:1 (Figures 2D and 2E). We found that ORF52 could also inhibit the enzymatic activity of mouse cGAS (mcGAS) in a dose-dependent manner (Figure 2F). These results indicate that ORF52 directly inhibits cGAS enzymatic activity, resulting in decreased cGAMP synthesis.

### DNA Binding Is Required for ORF52 to Inhibit cGAS Activity

Because cGAS activity depends on DNA, we performed assays with increasing concentration of ISD (up to a DNA:cGAS molar ratio of 30:1) in the presence or absence of ORF52 (ORF52:cGAS of 4:1). At low-intermediate concentrations of DNA, cGAS activity was completely inhibited by ORF52 (Figure 3A). However, at high concentrations of DNA (DNA:cGAS molar ratio of >4:1), the inhibition of cGAS activity by ORF52 could be partially overcome. To further quantify the effect of ORF52 on cGAS activity, we plotted the multiple turnover reaction rate at a given cGAS concentration against the concentration of DNA in order to obtain the EC $_{50}$  value of DNA (the concentration of DNA at which cGAS reaches half its maximum activity). The EC $_{50}$  was significantly greater when 4  $\mu$ M ORF52 was present (7.65  $\mu$ M) than when it was absent (0.05  $\mu$ M) (Figure 3A), suggesting that ORF52 may sequester DNA from cGAS.

However, cGAS apparently binds to DNA more efficiently than ORF52, as revealed by fluorescence polarization DNA binding assay (Figure 3B), raising the question of whether ORF52 inhibits cGAS activity solely through DNA binding. To address the extent to which DNA sequestration contributes to cGAS inhibition, we screened ORF52 mutants deficient in DNA binding, using a DNA binding assay with dsDNA-coupled cellulose beads (Figure 3C, upper panel). We found that one ORF52 mutant (K68/69A) exhibited substantially reduced DNA binding ability (Figure 3C, lower panel, lane 14). We then examined inhibition of cGAS by ORF52-K68/69A and found that loss of DNA binding compromised inhibition, supporting the role of DNA binding by ORF52 in cGAS inhibition (Figure 3D).

### ORF52 Interacts with cGAS

Although ORF52 inhibited DNA-induced cGAS-cGAMP signaling, it had little effect on DNA-induced inflammasome responses

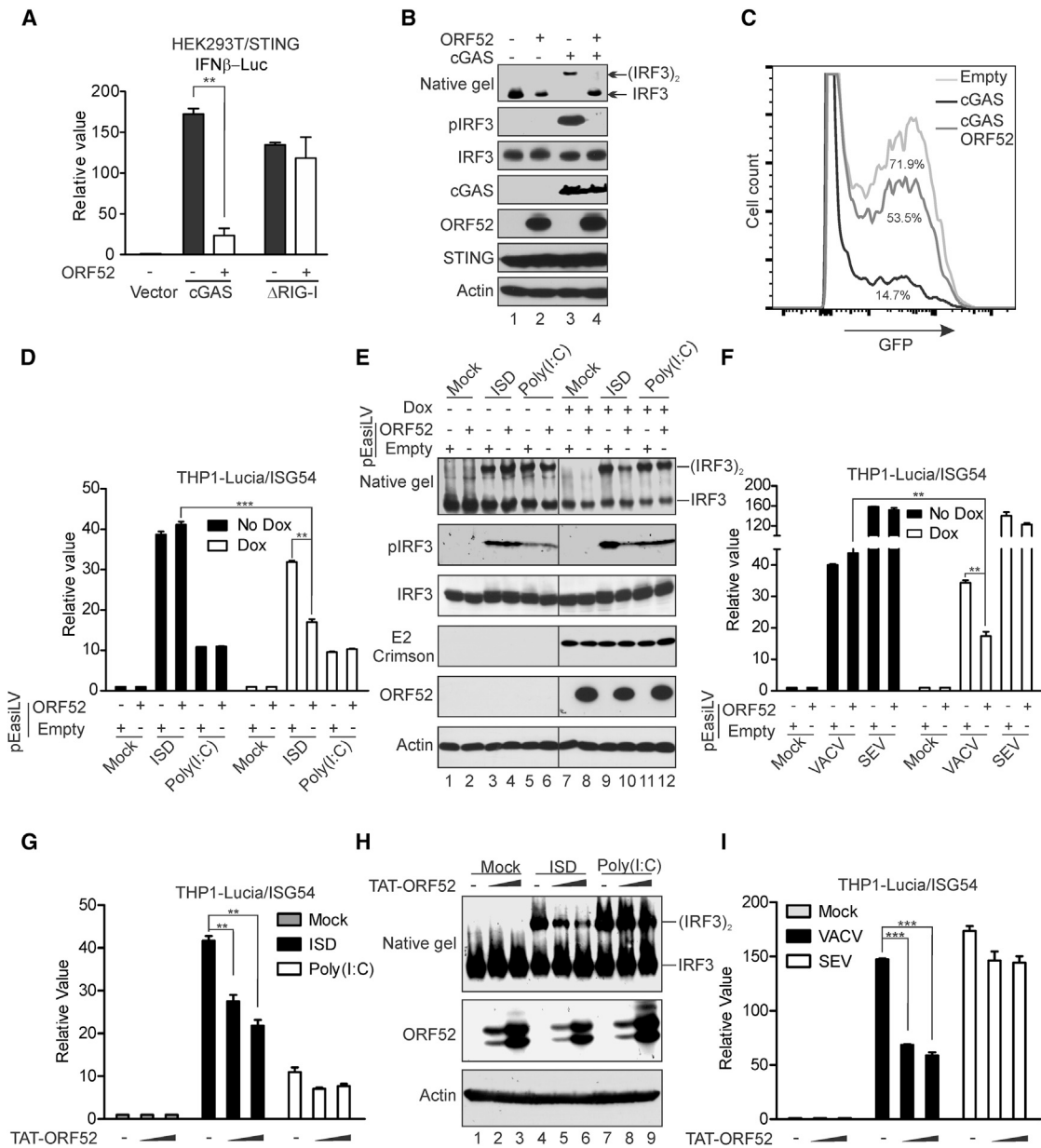


**Figure 1. Inhibition of cGAS DNA-Sensing Signaling by KSHV ORF52**

(A) KSHV ORF52 inhibits cGAS-induced IFN $\beta$  promoter activity. HEK293T-STING cells were transfected with IFN $\beta$  luciferase reporter and expression plasmids as indicated, and luciferase activity was assayed 24 hr after transfection. The relative luciferase activity was expressed as arbitrary units by normalizing firefly luciferase activity to Renilla luciferase activity.

(B) KSHV ORF52 inhibits cGAS-induced IRF3 dimerization and phosphorylation. HEK293T-STING cells were transfected with expression plasmids as indicated. Twenty-four hours after transfection, cell lysates were analyzed for IRF3 dimerization by native gel electrophoresis. IRF3 phosphorylation and expression levels of the transfected genes were monitored by immunoblotting with antibodies.

(C) KSHV ORF52 inhibits cGAS-induced antiviral response. HEK293T-STING cells transfected with specified plasmids were infected with vesicular stomatitis virus (VSV-GFP). The percentage of GFP-positive cells, as analyzed by FACS, is shown for each condition.

(D–F) ORF52 inhibits cGAS DNA sensing signaling in THP-1 cells. THP1 Lucia ISG cells harboring pEasiLV-ORF52 or pEasiLV-empty were untreated or induced with 2  $\mu$ g/ml doxycycline for 60 hr, then transfected with ISD45 or Poly(I:C) (2  $\mu$ g/ml) (D and E), or infected with VACV or SEV (F). The activity of secreted Lucia luciferase was determined, or cell lysates were harvested then analyzed for IRF3 dimerization and phosphorylation (E).

(G–I) TAT-ORF52 protein inhibits cGAS DNA-sensing signaling in THP-1 cells. THP1 Lucia ISG cells were incubated with 1.25  $\mu$ M or 2.5  $\mu$ M TAT-ORF52 protein for 3 hr, then transfected with ISD45 or Poly(I:C) (2  $\mu$ g/ml) (G and H) or infected with VACV or SEV (I). Analyses of luciferase activity or IRF3 dimerization were performed as in (D)–(F). \*\* $p$  < 0.01 and \*\*\* $p$  < 0.001; Student's  $t$  test. See also [Figures S1](#) and [S2](#).

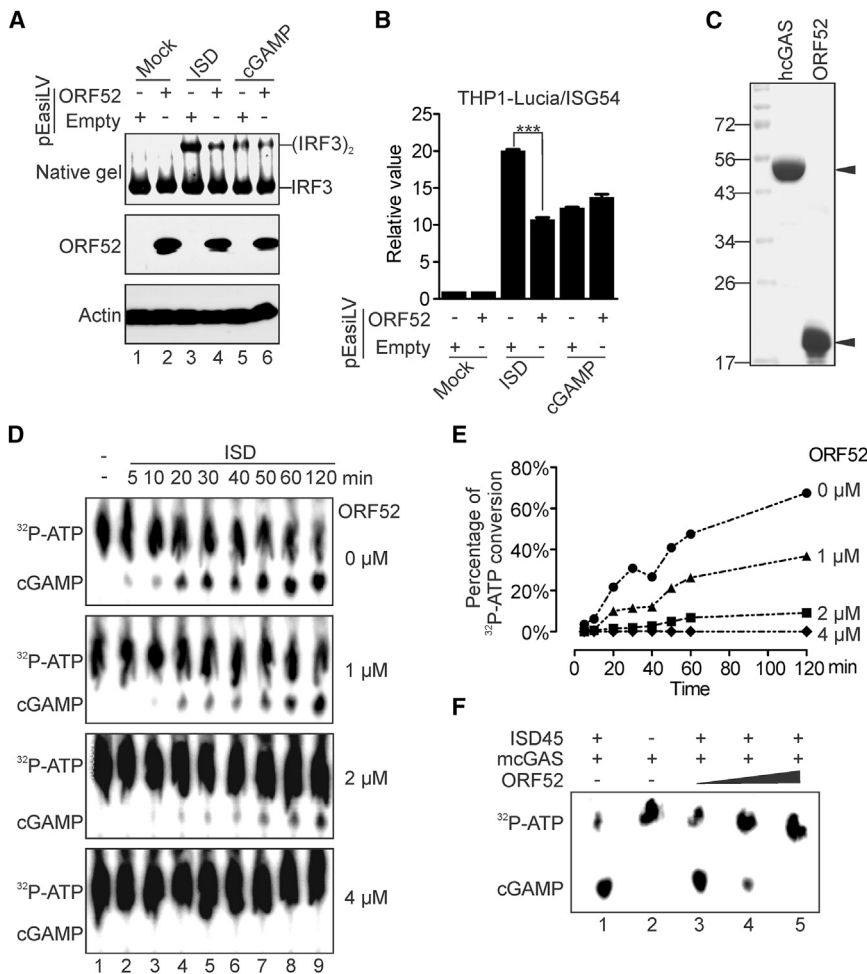


**Figure 2. ORF52 Inhibits cGAS Enzymatic Activity**

(A and B) ORF52 affects the cGAS-DNA-sensing signaling pathway upstream of cGAMP. THP1 Lucia ISG cells harboring pEasiLV-ORF52 or pEasiLV-empty were induced with 2  $\mu$ g/ml doxycycline for 60 hr, then transfected with ISD45 or cGAMP (2  $\mu$ g/ml). IRF3 dimerization was analyzed (A) or the secreted Lucia activity was determined (B) as in Figure 1.

(C) Coomassie blue staining of purified hcGAS and ORF52 proteins.

(D and E) ORF52 inhibits hcGAS enzymatic activity. Purified hcGAS protein (1  $\mu$ M) was incubated with ISD45 (1  $\mu$ M), [ $\alpha$ - $^{32}$ P]-ATP, ATP, and GTP in reaction buffer containing different amount of ORF52 protein (0, 1, 2, or 4  $\mu$ M). The reactions were stopped at the indicated time by boiling for 5 min. Synthesis of cGAMP was analyzed by thin-layer chromatography (TLC) (D), and the efficiency of cGAMP production was plotted against time (E).

(F) ORF52 inhibits mouse cGAS activity. Mouse cGAS (mcGAS; 1  $\mu$ M) was used for the enzyme assay and TLC as described in (D). \*\*\* $p$  < 0.001; Student's  $t$  test.

mediated by another cytosolic DNA sensor, AIM2 (Figures S3A and S3B) (Bürckstümmer et al., 2009; Fernandes-Alnemri et al., 2009; Hornung et al., 2009). The specific inhibition of cGAS by ORF52 prompted us to investigate the possibility of an interaction between the two proteins. Indeed, we found that GST-ORF52 pulled down Flag-tagged hcGAS efficiently, but not Flag-AIM2 under the same conditions (Figure 4A). The interaction between ORF52 and cGAS was evidently not dependent on DNA or RNA, because treatment with Benzonase, an enzyme that digests both DNA and RNA, or inclusion of ethidium bromide (EB), had little effect on it (Figure 4B). Importantly, ORF52 and cGAS also interact with each other in cells, as revealed by their coimmunoprecipitation (Figure 4C) and subcellular colocalization (Figure S3C). To further study their interactions, we mapped the interaction domains using a series of internal 10 aa deletion mutants of GST-ORF52 in GST pull-down assays and found that loss of aa 111–120 in ORF52 (ORF52  $\Delta$ 111–120) abolished its binding to cGAS (Figure 4D), which was confirmed by coimmunoprecipitation assays (Figure S3D). This deletion also compromised the inhibition of cGAS by ORF52 (Figure 3D). The K68/69A and  $\Delta$ 111–120 double mutant further reduced inhibition of cGAS (Figure 3D), supporting the idea that ORF52 blocks cGAS activity in part through their interaction. When expressed ectopically in THP-1 cells, ORF52 inhibited DNA-

induced dimerization and phosphorylation of IRF3, but ORF52 mutants deficient in cGAS- or DNA-binding exhibited reduced inhibition (Figure 4E). Similar results were obtained in HEK293T/STING cells (Figure 4F), and in THP-1 cells transfected with TAT-ORF52 WT or mutant protein (Figures S3E–S3G). These results corroborate our in vitro assays, suggesting that optimal inhibition of cGAS activity

requires both the cGAS-binding and DNA-binding properties of ORF52.

Interestingly, the cGAS-binding mutant, ORF52  $\Delta$ 111–120, also shows weakened DNA binding activity similar to that of K68/69A ( $K_d$  of 2.23 versus 2.21  $\mu$ M) (Figure S4A), making it difficult to distinguish the contributions of protein-protein and protein-DNA interactions from the loss of cGAS inhibition. We therefore mapped regions of cGAS involved in its interaction with ORF52. Our results showed that regions between aa 1–160 and aa 212–382 were involved in binding to ORF52 (Figure S4B). Consistently, we found that ORF52 inhibited the activity of the full-length cGAS more efficiently than the truncated form (aa 161–522) (Figures S4C–S4E).

### ORF52 Homologs Also Inhibit cGAS

ORF52 is a gammaherpesvirus-specific tegument protein (Bortz et al., 2003; Johannsen et al., 2004; O'Connor and Kedes, 2006; Zhu et al., 2005) and shares a high degree of conservation among them (Figure S5A). To investigate whether ORF52 homologs from other gammaherpesviruses also inhibit cGAS activity, we expressed them in bacteria and purified them to homogeneity (Figure S5B). Our in vitro enzymatic assay showed that these ORF52 homologs also inhibited cGAS activity (Figure 5A), and that they inhibited cGAS-dependent activation of IRF3 in cells

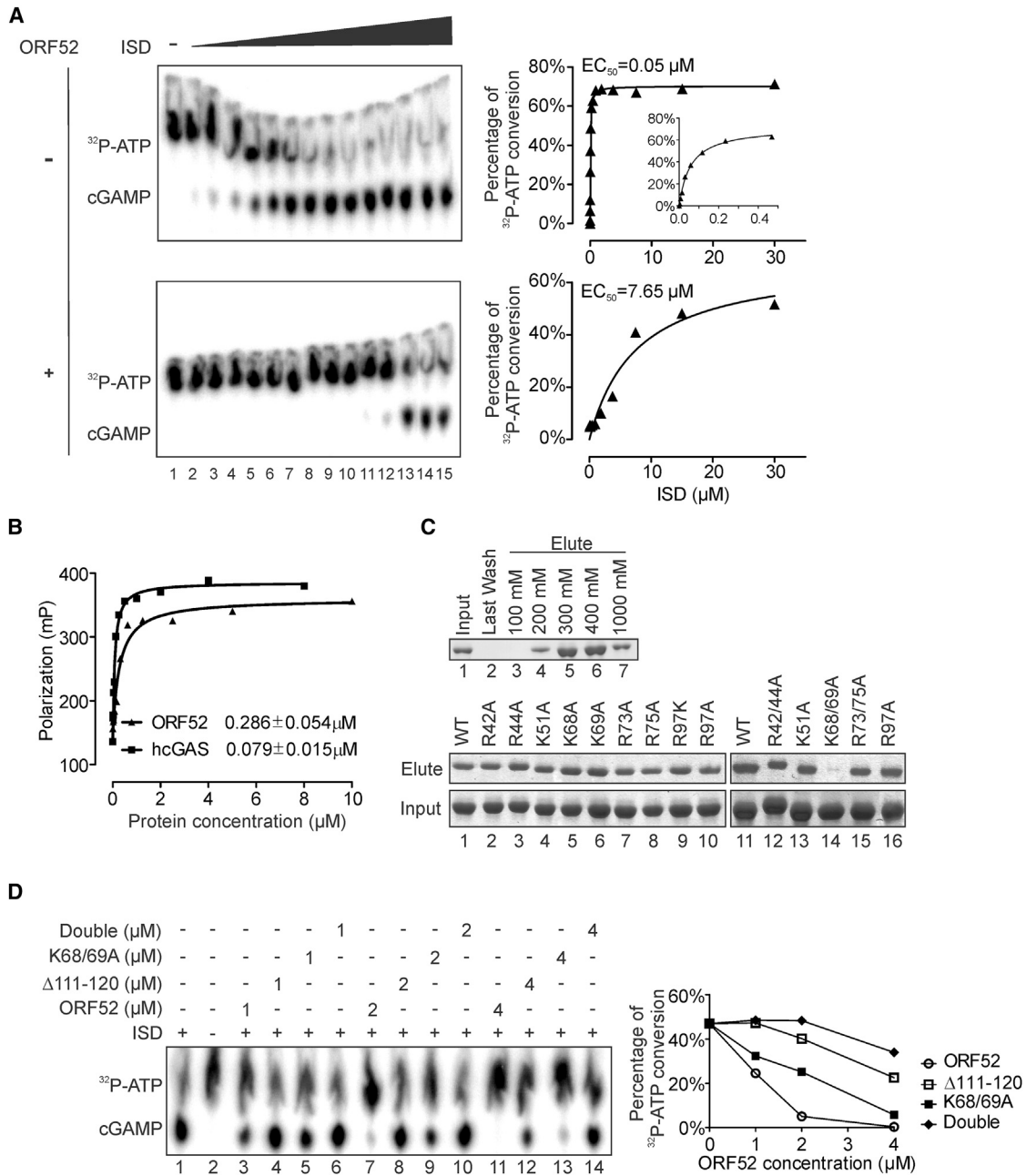


**Figure 3. ORF52 Binding to DNA Is Required for Its Inhibition of cGAS Activity**

(A) ORF52 affects the kinetics of cGAS-dependent cGAMP production. In vitro enzyme assay was performed as in Figure 2D with 2-fold serial dilutions of ISD45 (starting from 30 μM, from right to left) in the presence or absence of ORF52 (4 μM) for 2 hr. cGAMP production was detected by TLC, and the initial reaction velocity was plotted against substrate concentration together with least-squares fit to the Michaelis-Menten equation.

(B) Fluorescence polarization analysis of hcGAS or ORF52 binding to DNA. FAM-labeled ISD45 was incubated with different amounts of ORF52 or hcGAS protein, and the  $K_d$  values were obtained from least-squares fit to a hyperbolic binding isotherm.

(C) Mutagenesis of ORF52 reveals that K68/69 are critical for its binding to DNA. GST-ORF52 protein was pulled down by dsDNA cellulose beads, and then eluted with the indicated salt concentration (upper panel). The GST-ORF52 charge-deficient mutants were pulled down by dsDNA cellulose beads, eluted with 300 mM NaCl, separated by SDS-PAGE, and visualized by Coomassie staining.

(D) ORF52 mutants deficient in cGAS/DNA-binding display reduced inhibition of cGAS activity. In vitro enzyme assay was performed in the presence or absence of the indicated amount of ORF52 wild-type or mutant proteins, and the percentage of cGAMP production was plotted for each protein concentration (right panel). See also Figure S3.







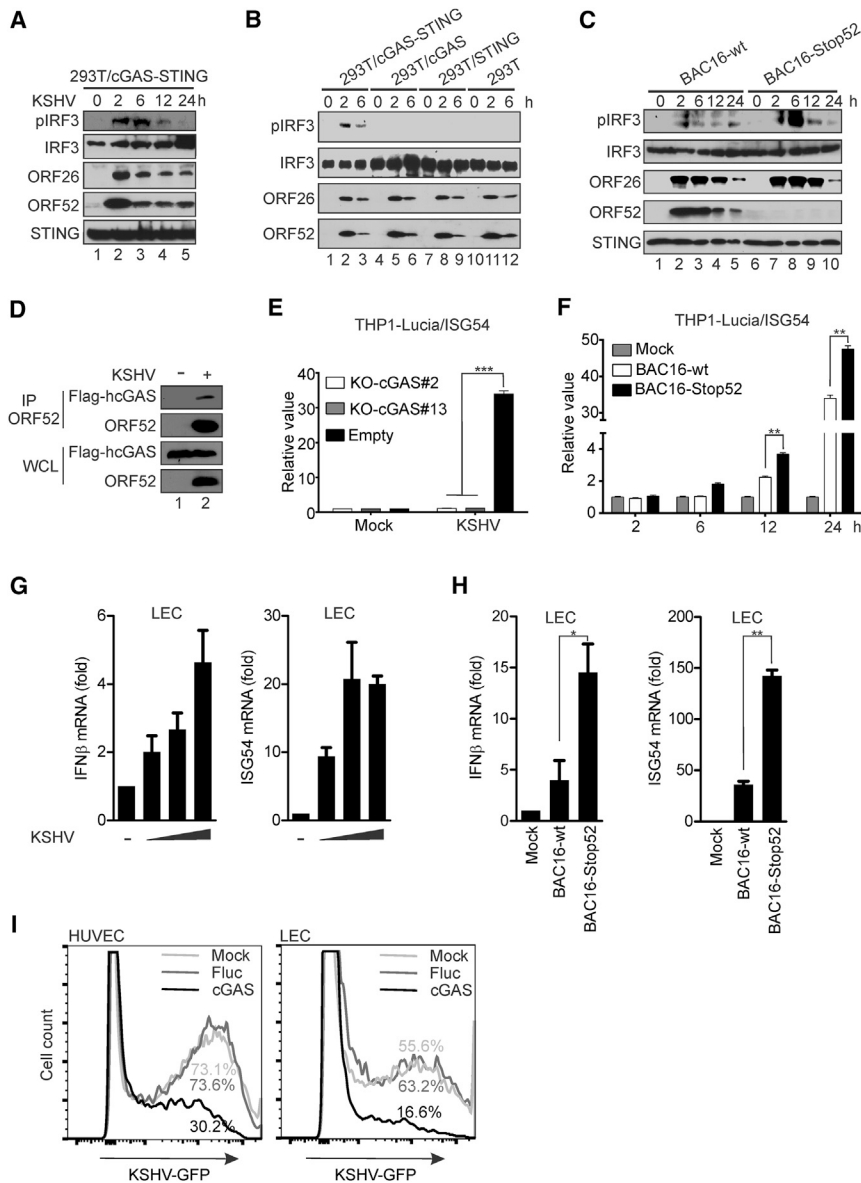


**Figure 6. KSHV ORF52 Antagonizes cGAS-Dependent Induction of the Innate Immune Response to Primary Infection**

(A) HEK293T/cGAS-STING cells were infected by KSHV. At the indicated time after infection, cell lysates were analyzed by western blotting with the indicated antibodies.

(B) KSHV primary infection and analysis of the indicated cell lines was performed as in (A).

(C) HEK293T/cGAS-STING cells were infected by KSHV BAC16-wt or BAC16-Stop52 mutant. At the indicated time after infection, cell lysates were analyzed by western blotting with the indicated antibodies.

(D) Flag-cGAS/293T cells were infected with KSHV at 50 genome copies/cell for 30 min, and then cell lysates were prepared and immunoprecipitated with anti-ORF52 4H4 antibody. The immunocomplexes were analyzed by western blot with indicated antibodies.

(E) cGAS was knocked out by CRISPR/Cas9-mediated genome editing in THP1 Lucia ISG cells. The knockout cell line and control were infected by KSHV, and the activity of secreted Lucia luciferase was assessed at 24 hpi.

(F) THP-1 Lucia ISG cells were infected by KSHV BAC16-wt or BAC16-Stop52 mutant. Luciferase activity was measured as in (E).

(G) LECs were mock treated or infected by KSHV at 25, 50, or 100 genome copies/cell. RNAs were isolated from cells and reverse transcribed. The levels of IFN $\beta$  and ISG54 mRNA were measured by qRT-PCR at 6 hpi.

(H) LECs were infected by KSHV BAC16-wt or BAC16-Stop52 at 50 copies/cell. The levels of IFN $\beta$  and ISG54 mRNA were measured as in (G).

(I) HUVECs or LECs were transduced with lentiviruses as indicated. At 24 hr after transduction, they were infected with BAC16-wt, followed by fixation and FACS analyses of the GFP-positive cells the next day. \*p < 0.05 and \*\*p < 0.01; Student's t test. See also Figure S6.

and, most importantly, that ORF52 directly inhibited cGAS enzymatic activity. Although ORF52 binds to DNA, no known DNA binding domain can be recognized. Unlike most DNA-binding proteins that are usually localized in the nucleus, ORF52 is found exclusively in the cytoplasm (Figure S3C; Sander et al., 2008), a feature that might play an important role in the inhibition of cGAS. Although the DNA-binding capacity of ORF52 is required for inhibition of cGAS, it is apparently insufficient because ORF52 binds to DNA with less affinity than cGAS. Importantly, we found ORF52 also bound to cGAS, but not to another cytosolic DNA sensor, AIM2. This difference explains why ORF52 inhibits cGAS-dependent activation of IRF3 but not AIM2-dependent inflammasome responses. The fact the AIM2 DNA binding domain cannot inhibit cGAS either in vitro or in vivo reaffirms that simple sequestration of DNA appears not to be an effective mechanism of inhibiting cGAS. Interestingly, ORF52 binds to

both the catalytic domains aa 212–382 and aa 1–160, which appears to be a regulatory domain of cGAS (Sun et al., 2013).

Unfortunately, because the DNA- and cGAS-binding properties of ORF52 are seemingly inseparable, the extent to which they contribute to the inhibition of cGAS is unknown. Nevertheless, our data suggest both DNA-binding and cGAS-binding are required for inhibition of cGAS by ORF52. Further structural studies of ORF52 interaction with cGAS and/or DNA will be crucial for delineation of the underlying molecular mechanisms.

Although ORF52 efficiently inhibits cGAS activity, ORF52 null mutant viruses only resulted in a moderate increase in IRF3-dependent responses. This is not surprising, because KSHV is known to encode multiple genes of immune modulatory functions, and because our initial screening found at least eight ORFs that interfered with the cGAS-STING signaling pathway. Some of these have been shown to subvert innate immunity by means of diverse mechanisms. But, unlike ORF52 that targets cGAS directly, these KSHV proteins appear to interfere with

downstream signaling components of cGAS, including IRFs. For example, K9 (vIRF-1), ORF36, and ORF45 all interfere with activation of IRFs (Gao et al., 1997; Hwang et al., 2009; Liang et al., 2012; Lin et al., 2001; Sathish and Yuan, 2011; Zhu et al., 2002); ORF64, a viral deubiquitinase (DUB), interferes with ubiquitination of the key components of innate immune signaling pathways (Inn et al., 2011; Wang et al., 2013). Because many viral immunomodulatory proteins are known to interfere with different aspects of immune responses, we expect that further studies will reveal additional roles and mechanisms by which these KSHV proteins subvert the host antiviral immune responses. The rich presence of antagonists of pattern recognition receptors (PRRs) provides an ideal mechanism to suppress activation of sensing of virion-contained PAMPs, thus blocking the upregulation of the next wave of ISGs.

Although ORF52 is known as an abundant tegument protein in virions (Bortz et al., 2007; Johannsen et al., 2004; O'Connor and Kedes, 2006; Zhu et al., 2005), its precise function has remained elusive (Anderson et al., 2014; Bortz et al., 2007; Wang et al., 2012). It is conserved among gammaherpesviruses but not in alpha or beta herpesviruses. Significantly, we found that ORF52 homologs also bound to cGAS and DNA and inhibited cGAS activity directly, suggesting that inhibition of cGAS by virion-contained ORF52 is a conserved mechanism for gammaherpesviruses.

Viral inhibitors of RNA sensing have been extensively studied, and several viral strategies to avoid dsRNA-mediated activation of RNA sensors have been characterized (Gack, 2014; Yoneyama et al., 2015; Zinzula and Tramontano, 2013). We show here that ORF52 is a viral inhibitor of the principal cytosolic DNA sensor, cGAS. We propose to name it KSHV inhibitor of cGAS (KicGAS). A growing number of viruses and bacteria have been shown to be sensed by cGAS (Dai et al., 2014; Gao et al., 2013a; Lam et al., 2014; Li et al., 2013b; Collins et al., 2015; Hansen et al., 2014; Storek et al., 2015; Wassermann et al., 2015; Watson et al., 2015). Among hundreds of ISGs evaluated by Dr. Charles Rice's group, cGAS is one of the few that exhibit potent antiviral effects on diverse groups of both DNA and RNA viruses (Schoggins et al., 2011, 2014). Viruses other than gammaherpesviruses are conceivably expected to encode cGAS antagonists. A recent study has revealed that the HSV-1 VP22 core domain has limited structural and sequence homology to MHV68 ORF52 (Hew et al., 2015). Because VP22 is also an abundant tegument protein (Spear and Roizman, 1972), it would be interesting to examine whether VP22 can inhibit cGAS, and how other large DNA viruses, such as alpha and beta herpesviruses and poxviruses, overcome cGAS-dependent DNA sensing. Collectively, our results have provided insights into the study of viral strategies to antagonize cGAS DNA-sensing signaling. The sensing of self and foreign DNA is delicately regulated (Ablasser et al., 2014; Konno et al., 2013; Liang et al., 2014), and the dysregulation of DNA sensing is associated with several human autoimmune diseases, such as systemic lupus erythematosus and Aicardi-Goutières syndrome (Ahn and Barber, 2014). Therefore, further delineation of the mechanisms by which KicGAS inhibits cGAS will aid in our understanding of this pathway, and may facilitate the development of therapeutics to treat or prevent diseases in which this pathway is dysregulated.

## EXPERIMENTAL PROCEDURES

### Cell Culture and Transfection

HEK293T and HeLa cells were cultured under 5% CO<sub>2</sub> at 37°C in Dulbecco's modified Eagle's medium (DMEM) supplemented with 10% fetal bovine serum (FBS) and antibiotics. iSLK-puro cells carrying BAC16 wild-type or mutants were cultured in DMEM containing 10% FBS, 50 µg/ml G418, 1 µg/ml puromycin, and 500 µg/ml hygromycin (Brulois et al., 2012; Myoung and Ganem, 2011). Conditions for induction of lytic reactivation in these cells were described previously (Fu et al., 2015). THP-1 and THP1 Lucia ISG cells (InvivoGen) were cultured in RPMI containing 10% FBS, and antibiotics. LECs and HUVECs were cultured in EBM-2 media supplemented with the EGM-2 MV bullet in collagen type I-coated dishes. Transient transfections were performed with Lipofectamine 2000 according to the manufacturer's protocol, or with polyethylenimine (PEI), or calcium chloride using standard protocols.

### Luciferase Reporter Assays

HEK293T/STING cells seeded on 24-well plates were transiently transfected with 100 ng of the luciferase reporter plasmid together with a total of 300 ng of various expression plasmids and/or empty vector controls using Effectene Transfection Reagent (QIAGEN). As an internal control, 10 ng of pRL-TK (Renilla luciferase) was transfected simultaneously. Luciferase assays were then performed at 24 hr posttransfection according to the Promega Dual-Luciferase Reporter Assay System protocol. The relative luciferase activity was expressed as arbitrary units by normalizing firefly to Renilla luciferase activity.

### Induction of Immune Responses by Nucleic Acid Transfection and Virus Infection

HEK293T or SLK cells were mock treated or transfected with ISD or Poly(I:C) (2 µg/ml). THP1-Lucia ISG cells carrying ORF52-pEasiLV or Empty-pEasiLV were untreated or treated with doxycycline (2 µg/ml) for 60 hr, then seeded to new wells and either mock treated or transfected with ISD/Poly(I:C) (2 µg/ml) or cGAMP (2 µg/ml; Figures 2A and 2B). Six hours posttransfection, cell lysates were harvested and analyzed by native PAGE (to detect IRF3 dimerization) or western blot. Alternatively, the media was collected at 16 hr posttransfection, and the activity of secreted Lucia luciferase was determined by addition of QUANTI-Luc (InvivoGen) and analysis with a luminometer. To detect the immune response to virus infection, HEK293T cells were mock infected or infected with VACV, or SEV. THP1-Lucia cells carrying ORF52-pEasiLV or Empty-pEasiLV were mock treated or treated with doxycycline, then infected with VACV or SEV. Analysis of IRF3 activation and luciferase assay were performed as described above.

### Protein Purification

TAT-ORF52 protein purification was performed according to Dr. S.F. Dowdy's group (Becker-Hapak and Dowdy, 2003). Further details, including methods used to purify His-tagged cGAS and ORF52, can be found in the [Supplemental Information](#).

### TAT-ORF52 Protein Transduction

THP1-Lucia cells were incubated with TAT-ORF52 proteins (1.25 or 2.5 µM) in serum-free media. After 3 hr, cells were washed with complete media (RPMI + 10% FBS), then either transfected with ISD/Poly(I:C) or infected with VACV/SEV virus as described above. Delivery of protein into cells was confirmed by immunofluorescence staining using anti-ORF52 antibody.

### GST Pull-Down Assay

GST-ORF52 or mutant proteins were bound to glutathione agarose beads, and incubated for 3 hr with lysates from HEK293T cells transiently expressing Flag-cGAS or Flag-AIM2. The beads were washed three times each with whole-cell lysis (WCL) buffer (50 mM Tris-HCl [pH 7.4], 150 mM NaCl, 1% NP-40, 1 mM sodium orthovanadate [Na<sub>3</sub>VO<sub>4</sub>], 40 mM-glycerophosphate, 1 mM sodium fluoride, 10% glycerol, 5 mM EDTA, 5 µg/ml of aprotinin, 5 µg/ml of leupeptin, 5 mM benzamide, and 1 mM PMSF) and 1 × PBS, then mixed with an equal volume of 2 × Laemmli loading buffer, and boiled for 10 min. The input/eluates

were resolved by SDS-PAGE and analyzed by Coomassie staining and/or western blot.

### In Vitro Enzyme Assay

cGAS protein was incubated with ISD45, 100  $\mu$ M ATP, 100  $\mu$ M GTP,  $\alpha$ - $^{32}$ P-ATP (10  $\mu$ Ci), and the indicated amount of ORF52 protein in reaction buffer at 37°C for the indicated time. The reaction was terminated by boiling for 5 min. Of each sample, 1  $\mu$ L was applied to a PEI-Cellulose F thin-layer chromatography plate. Reaction products were resolved with 1 M  $(\text{NH}_4)_2\text{SO}_4$ /1.5 M  $\text{KH}_2\text{PO}_4$  (pH 3.8). Plates were dried at 80°C for 10 min, and radiolabeled products were detected by a Storm phosphorimager (GE Life Sciences). The signal was analyzed with ImageQuant, and the data were fitted to a Michaelis-Menten-like equation:  $Y = V_{\text{max}} \cdot [\text{ISD45}] / (\text{EC}_{50} + [\text{ISD45}])$ . The  $\text{EC}_{50}$  value of DNA determined in this manner indicated the concentration of DNA at which cGAS reaches its half-maximum activity. Detailed experimental procedures are shown in the [Supplemental Information](#).

### Double-Stranded DNA Cellulose Pull-Down Assay

dsDNA cellulose (Sigma, D8515) was incubated with purified GST-ORF52 or mutant proteins in buffer (50 mM Tris-HCl [pH 7.4], 100 mM NaCl, 1 mM sodium orthovanadate  $[\text{Na}_3\text{VO}_4]$ , 1  $\times$  protease inhibitor cocktail, and 1 mM PMSF) for 1 hr at 4°C, then washed three times with the same buffer. The protein bound beads were eluted stepwise with 10 mM Tris-HCl (pH 7.4) buffer containing different concentrations of NaCl ([Figure 3C](#), upper panel), buffer containing 300 mM NaCl ([Figure 3C](#), lower panel), or with 2  $\times$  Laemmli loading buffer ([Figure 5D](#)). The input and eluted proteins were then applied to SDS-PAGE and stained by Coomassie blue.

### Virus Stock Preparation and Infection

For KSHV, virus stock preparation, quantification, and infection were performed as described previously ([Fu et al., 2015](#)). SEV was used at a final concentration of 50 HA units/ml. VACV was inactivated at 56°C for 30 min before usage and was used at an moi of 10. For vesicular stomatitis virus infection, VSV-GFP was used at an moi of 1. Cells were analyzed by FACS at 48 hr postinfection. Further details can be found in the [Supplemental Information](#).

### Quantitative Real-Time PCR Analysis

LECs were mock treated or infected with KSHV for 6 hr. The mRNA was extracted, reverse transcribed, and mRNA levels determined by real-time PCR. Expression levels were normalized to GAPDH expression and data are presented as fold induction over mock treatment control. More details can be found in the [Supplemental Information](#).

### CRISPR/Cas9-Mediated Genome Editing

Potential guide RNAs (gRNAs) targeting the first exon of cGAS were analyzed using the CRISPR Design tool ([crispr.mit.edu](http://crispr.mit.edu)). Double-stranded oligos were cloned into the lentiCRISPRv1 vector and cotransfected with packaging plasmids into HEK293T cells. Lentiviral particles were collected and used to transduce THP1 Lucia ISG cells. #2 and #13 represent two single-cell clones with efficient cGAS knockout. More details regarding generation and validation of these cell lines can be found in the [Supplemental Information](#).

### SUPPLEMENTAL INFORMATION

Supplemental Information includes six figures and Supplemental Experimental Procedures and can be found with this article at <http://dx.doi.org/10.1016/j.chom.2015.07.015>.

### AUTHOR CONTRIBUTIONS

J.-j.W., W.L., and F.Z. designed the experiments and analyzed the data. J.-j.W., W.L., Y.S., D.A., B.F., J.G., T.H., S.M., and X.L. performed the experiments. J.-j.W., W.L., D.A., H.L., and F.Z. wrote the paper. A.K., F.N., M.S., W.M., and D.W. provided some reagents.

### ACKNOWLEDGMENTS

We thank Drs. Kevin Brulois, Katherine Fitzgerald, Adolfo Garcia-Sastre, David Gilbert, Young-Kwon Hong, Pingwei Li, Michael Malim, Jinjong Myoung, Charles Rice, Ren Sun, Hengli Tang, Scott Wong, and Feng Zhang for reagents. We thank the Florida State University hybridoma facility for generating anti-ORF52 antibodies. We thank Dr. Lijun Sun for his helpful advice regarding the IRF3 dimerization assay. We also thank Ms. Jen Kennedy at the Florida State University for editorial assistance. We thank Drs. Betty Gaffney, Kenneth Roux, Beth Stroupe, and Hengli Tang and all members of the Zhu lab for helpful comments and discussion. This work was supported by NIH grants R01 DE016680 (to F.Z.), F31 CA183250 (to D.A.), and R01 GM099604 and R01 GM66958 (to H.L.) and in part by the National Cancer Institute, NIH (contract number HHSN26120080001E).

Received: March 31, 2015

Revised: June 16, 2015

Accepted: July 30, 2015

Published: August 27, 2015

### REFERENCES

- Ablasser, A., Goldeck, M., Cavlari, T., Deimling, T., Witte, G., Röhl, I., Hopfner, K.-P., Ludwig, J., and Hornung, V. (2013a). cGAS produces a 2'-5'-linked cyclic dinucleotide second messenger that activates STING. *Nature* **498**, 380–384.
- Ablasser, A., Schmid-Burgk, J.L., Hemmerling, I., Horvath, G.L., Schmidt, T., Lutz, E., and Hornung, V. (2013b). Cell intrinsic immunity spreads to bystander cells via the intercellular transfer of cGAMP. *Nature* **503**, 530–534.
- Ablasser, A., Hemmerling, I., Schmid-Burgk, J.L., Behrendt, R., Roers, A., and Hornung, V. (2014). TREX1 deficiency triggers cell-autonomous immunity in a cGAS-dependent manner. *J. Immunol.* **192**, 5993–5997.
- Ahn, J., and Barber, G.N. (2014). Self-DNA, STING-dependent signaling and the origins of autoinflammatory disease. *Curr. Opin. Immunol.* **31**, 121–126.
- Anderson, M.S., Loftus, M.S., and Kedes, D.H. (2014). Maturation and vesicle-mediated egress of primate gammaherpesvirus rhesus monkey rhadinovirus require inner tegument protein ORF52. *J. Virol.* **88**, 9111–9128.
- Barber, G.N. (2014). STING-dependent cytosolic DNA sensing pathways. *Trends Immunol.* **35**, 88–93.
- Becker-Hapak, M., and Dowdy, S.F. (2003). Protein transduction: generation of full-length transducible proteins using the TAT system. *Curr. Protoc. Cell Biol.* **18**, <http://dx.doi.org/10.1002/0471143030.cb2002s18>.
- Bortz, E., Whitelegge, J.P., Jia, Q., Zhou, Z.H., Stewart, J.P., Wu, T.-T., and Sun, R. (2003). Identification of proteins associated with murine gammaherpesvirus 68 virions. *J. Virol.* **77**, 13425–13432.
- Bortz, E., Wang, L., Jia, Q., Wu, T.-T., Whitelegge, J.P., Deng, H., Zhou, Z.H., and Sun, R. (2007). Murine gammaherpesvirus 68 ORF52 encodes a tegument protein required for virion morphogenesis in the cytoplasm. *J. Virol.* **81**, 10137–10150.
- Brulois, K.F., Chang, H., Lee, A.S.-Y., Ensser, A., Wong, L.-Y., Toth, Z., Lee, S.H., Lee, H.-R., Myoung, J., Ganem, D., et al. (2012). Construction and manipulation of a new Kaposi's sarcoma-associated herpesvirus bacterial artificial chromosome clone. *J. Virol.* **86**, 9708–9720.
- Bürkstümmer, T., Baumann, C., Blüml, S., Dixit, E., Dürnberger, G., Jahn, H., Planyavsky, M., Bilban, M., Colinge, J., Bennett, K.L., and Superti-Furga, G. (2009). An orthogonal proteomic-genomic screen identifies AIM2 as a cytoplasmic DNA sensor for the inflammasome. *Nat. Immunol.* **10**, 266–272.
- Cai, X., Chiu, Y.H., and Chen, Z.J. (2014). The cGAS-cGAMP-STING pathway of cytosolic DNA sensing and signaling. *Mol. Cell* **54**, 289–296.
- Cesarman, E., Chang, Y., Moore, P.S., Said, J.W., and Knowles, D.M. (1995). Kaposi's sarcoma-associated herpesvirus-like DNA sequences in AIDS-related body-cavity-based lymphomas. *N. Engl. J. Med.* **332**, 1186–1191.
- Chang, Y., Cesarman, E., Pessin, M.S., Lee, F., Culpepper, J., Knowles, D.M., and Moore, P.S. (1994). Identification of herpesvirus-like DNA sequences in AIDS-associated Kaposi's sarcoma. *Science* **266**, 1865–1869.

- Civril, F., Deimling, T., de Oliveira Mann, C.C., Ablasser, A., Moldt, M., Witte, G., Hornung, V., and Hopfner, K.-P. (2013). Structural mechanism of cytosolic DNA sensing by cGAS. *Nature* *498*, 332–337.
- Collins, A.C., Cai, H., Li, T., Franco, L.H., Li, X.D., Nair, V.R., Scharn, C.R., Stamm, C.E., Levine, B., Chen, Z.J., and Shiloh, M.U. (2015). Cyclic GMP-AMP synthase is an innate immune DNA sensor for *Mycobacterium tuberculosis*. *Cell Host Microbe* *17*, 820–828.
- Dai, P., Wang, W., Cao, H., Avogadri, F., Dai, L., Drexler, I., Joyce, J.A., Li, X.-D., Chen, Z., Merghoub, T., et al. (2014). Modified vaccinia virus Ankara triggers type I IFN production in murine conventional dendritic cells via a cGAS/STING-mediated cytosolic DNA-sensing pathway. *PLoS Pathog.* *10*, e1003989.
- Fernandes-Alnemri, T., Yu, J.-W., Datta, P., Wu, J., and Alnemri, E.S. (2009). AIM2 activates the inflammasome and cell death in response to cytoplasmic DNA. *Nature* *458*, 509–513.
- Fu, B., Kuang, E., Li, W., Avey, D., Li, X., Turpin, Z., Valdes, A., Brulois, K., Myoung, J., and Zhu, F. (2015). Activation of p90 ribosomal S6 kinases by ORF45 of Kaposi's sarcoma-associated herpesvirus is critical for optimal production of infectious viruses. *J. Virol.* *89*, 195–207.
- Gack, M.U. (2014). Mechanisms of RIG-I-like receptor activation and manipulation by viral pathogens. *J. Virol.* *88*, 5213–5216.
- Ganem, D. (2007). Kaposi's sarcoma-associated herpesvirus. In *Fields Virology*, D.M. Knipe, P.M. Howley, D.E. Griffin, R.A. Lamb, M.A. Martin, B. Roizman, and S.E. Straus, eds. (Philadelphia: Lippincott Williams & Wilkins), pp. 2847–2888.
- Ganem, D. (2010). KSHV and the pathogenesis of Kaposi sarcoma: listening to human biology and medicine. *J. Clin. Invest.* *120*, 939–949.
- Gao, S.J., Boshoff, C., Jayachandra, S., Weiss, R.A., Chang, Y., and Moore, P.S. (1997). KSHV ORF K9 (vIRF) is an oncogene which inhibits the interferon signaling pathway. *Oncogene* *15*, 1979–1985.
- Gao, D., Wu, J., Wu, Y.-T., Du, F., Aroh, C., Yan, N., Sun, L., and Chen, Z.J. (2013a). Cyclic GMP-AMP synthase is an innate immune sensor of HIV and other retroviruses. *Science* *341*, 903–906.
- Gao, P., Ascano, M., Wu, Y., Barchet, W., Gaffney, B.L., Zillinger, T., Serganov, A.A., Liu, Y., Jones, R.A., Hartmann, G., et al. (2013b). Cyclic [G(2',5')pA(3',5')p] is the metazoan second messenger produced by DNA-activated cyclic GMP-AMP synthase. *Cell* *153*, 1094–1107.
- Gao, P., Ascano, M., Zillinger, T., Wang, W., Dai, P., Serganov, A.A., Gaffney, B.L., Shuman, S., Jones, R.A., Deng, L., et al. (2013c). Structure-function analysis of STING activation by c[G(2',5')pA(3',5')p] and targeting by antiviral DMXAA. *Cell* *154*, 748–762.
- Hansen, K., Prabakaran, T., Laustsen, A., Jørgensen, S.E., Rahbæk, S.H., Jensen, S.B., Nielsen, R., Leber, J.H., Decker, T., Horan, K.A., et al. (2014). *Listeria monocytogenes* induces IFN $\beta$  expression through an IFI16-, cGAS- and STING-dependent pathway. *EMBO J.* *33*, 1654–1666.
- Heine, J.W., Honess, R.W., Cassai, E., and Roizman, B. (1974). Proteins specified by herpes simplex virus. XII. The virion polypeptides of type 1 strains. *J. Virol.* *14*, 640–651.
- Hew, K., Dahlroth, S.L., Pan, L.X., Cornvik, T., and Nordlund, P. (2015). The core domain of VP22 from herpes simplex virus 1 reveals a surprising structural conservation in both the alpha and the gamma herpesvirus subfamilies. *J. Gen. Virol.*
- Horan, K.A., Hansen, K., Jakobsen, M.R., Holm, C.K., Søby, S., Unterholzner, L., Thompson, M., West, J.A., Iversen, M.B., Rasmussen, S.B., et al. (2013). Proteasomal degradation of herpes simplex virus capsids in macrophages releases DNA to the cytosol for recognition by DNA sensors. *J. Immunol.* *190*, 2311–2319.
- Hornung, V., Ablasser, A., Charrel-Dennis, M., Bauernfeind, F., Horvath, G., Caffrey, D.R., Latz, E., and Fitzgerald, K.A. (2009). AIM2 recognizes cytosolic dsDNA and forms a caspase-1-activating inflammasome with ASC. *Nature* *458*, 514–518.
- Hwang, S., Kim, K.S., Flano, E., Wu, T.-T., Tong, L.M., Park, A.N., Song, M.J., Sanchez, D.J., O'Connell, R.M., Cheng, G., and Sun, R. (2009). Conserved herpesviral kinase promotes viral persistence by inhibiting the IRF-3-mediated type I interferon response. *Cell Host Microbe* *5*, 166–178.
- Inn, K.-S., Lee, S.-H., Rathbun, J.Y., Wong, L.-Y., Toth, Z., Machida, K., Ou, J.-H.J., and Jung, J.U. (2011). Inhibition of RIG-I-mediated signaling by Kaposi's sarcoma-associated herpesvirus-encoded deubiquitinase ORF64. *J. Virol.* *85*, 10899–10904.
- Johannsen, E., Luftig, M., Chase, M.R., Weicksel, S., Cahir-McFarland, E., Illanes, D., Sarracino, D., and Kieff, E. (2004). Proteins of purified Epstein-Barr virus. *Proc. Natl. Acad. Sci. USA* *101*, 16286–16291.
- Konno, H., Konno, K., and Barber, G.N. (2013). Cyclic dinucleotides trigger ULK1 (ATG1) phosphorylation of STING to prevent sustained innate immune signaling. *Cell* *155*, 688–698.
- Kranzusch, P.J., Lee, A.S., Berger, J.M., and Doudna, J.A. (2013). Structure of human cGAS reveals a conserved family of second-messenger enzymes in innate immunity. *Cell Rep.* *3*, 1362–1368.
- Lam, E., Stein, S., and Falck-Pedersen, E. (2014). Adenovirus detection by the cGAS/STING/TBK1 DNA sensing cascade. *J. Virol.* *88*, 974–981.
- Li, X., Shu, C., Yi, G., Chaton, C.T., Shelton, C.L., Diao, J., Zuo, X., Kao, C.C., Herr, A.B., and Li, P. (2013a). Cyclic GMP-AMP synthase is activated by double-stranded DNA-induced oligomerization. *Immunity* *39*, 1019–1031.
- Li, X.D., Wu, J., Gao, D., Wang, H., Sun, L., and Chen, Z.J. (2013b). Pivotal roles of cGAS-cGAMP signaling in antiviral defense and immune adjuvant effects. *Science* *341*, 1390–1394.
- Liang, Q., Fu, B., Wu, F., Li, X., Yuan, Y., and Zhu, F. (2012). ORF45 of Kaposi's sarcoma-associated herpesvirus inhibits phosphorylation of interferon regulatory factor 7 by IKK $\epsilon$  and TBK1 as an alternative substrate. *J. Virol.* *86*, 10162–10172.
- Liang, Q., Seo, G.J., Choi, Y.J., Kwak, M.J., Ge, J., Rodgers, M.A., Shi, M., Leslie, B.J., Hopfner, K.P., Ha, T., et al. (2014). Crosstalk between the cGAS DNA sensor and Beclin-1 autophagy protein shapes innate antimicrobial immune responses. *Cell Host Microbe* *15*, 228–238.
- Lin, R., Genin, P., Mamane, Y., Sgarbanti, M., Battistini, A., Harrington, W.J., Jr., Barber, G.N., and Hiscott, J. (2001). HHV-8 encoded vIRF-1 represses the interferon antiviral response by blocking IRF-3 recruitment of the CBP/p300 coactivators. *Oncogene* *20*, 800–811.
- Myoung, J., and Ganem, D. (2011). Generation of a doxycycline-inducible KSHV producer cell line of endothelial origin: maintenance of tight latency with efficient reactivation upon induction. *J. Virol. Methods* *174*, 12–21.
- Nealon, K., Newcomb, W.W., Pray, T.R., Craik, C.S., Brown, J.C., and Kedes, D.H. (2001). Lytic replication of Kaposi's sarcoma-associated herpesvirus results in the formation of multiple capsid species: isolation and molecular characterization of A, B, and C capsids from a gammaherpesvirus. *J. Virol.* *75*, 2866–2878.
- O'Connor, C.M., and Kedes, D.H. (2006). Mass spectrometric analyses of purified rhesus monkey rhadinovirus reveal 33 virion-associated proteins. *J. Virol.* *80*, 1574–1583.
- Orzalli, M.H., and Knipe, D.M. (2014). Cellular sensing of viral DNA and viral evasion mechanisms. *Annu. Rev. Microbiol.* *68*, 477–492.
- Paludan, S.R., Bowie, A.G., Horan, K.A., and Fitzgerald, K.A. (2011). Recognition of herpesviruses by the innate immune system. *Nat. Rev. Immunol.* *11*, 143–154.
- Sander, G., Konrad, A., Thureau, M., Wies, E., Leubert, R., Kremmer, E., Dinkel, H., Schulz, T., Neipel, F., and Stürzl, M. (2008). Intracellular localization map of human herpesvirus 8 proteins. *J. Virol.* *82*, 1908–1922.
- Sathish, N., and Yuan, Y. (2011). Evasion and subversion of interferon-mediated antiviral immunity by Kaposi's sarcoma-associated herpesvirus: an overview. *J. Virol.* *85*, 10934–10944.
- Schoggins, J.W., Wilson, S.J., Panis, M., Murphy, M.Y., Jones, C.T., Bieniasz, P., and Rice, C.M. (2011). A diverse range of gene products are effectors of the type I interferon antiviral response. *Nature* *472*, 481–485.
- Schoggins, J.W., MacDuff, D.A., Imanaka, N., Gainey, M.D., Shrestha, B., Eitson, J.L., Mar, K.B., Richardson, R.B., Ratushny, A.V., Litvak, V., et al. (2014). Pan-viral specificity of IFN-induced genes reveals new roles for cGAS in innate immunity. *Nature* *505*, 691–695.

- Soulier, J., Grollet, L., Oksenhendler, E., Cacoub, P., Cazals-Hatem, D., Babinet, P., d'Agay, M.F., Clauvel, J.P., Raphael, M., Degos, L., et al. (1995). Kaposi's sarcoma-associated herpesvirus-like DNA sequences in multicentric Castlemann's disease. *Blood* 86, 1276–1280.
- Spear, P.G., and Roizman, B. (1972). Proteins specified by herpes simplex virus. V. Purification and structural proteins of the herpesvirion. *J. Virol.* 9, 143–159.
- Storek, K.M., Gertszvolf, N.A., Ohlson, M.B., and Monack, D.M. (2015). cGAS and Ifi204 cooperate to produce type I IFNs in response to *Francisella* infection. *J. Immunol.* 194, 3236–3245.
- Sun, L., Wu, J., Du, F., Chen, X., and Chen, Z.J. (2013). Cyclic GMP-AMP synthase is a cytosolic DNA sensor that activates the type I interferon pathway. *Science* 339, 786–791.
- Tanaka, Y., and Chen, Z.J. (2012). STING specifies IRF3 phosphorylation by TBK1 in the cytosolic DNA signaling pathway. *Sci. Signal.* 5, ra20.
- Wang, L., Guo, H., Reyes, N., Lee, S., Bortz, E., Guo, F., Sun, R., Tong, L., and Deng, H. (2012). Distinct domains in ORF52 tegument protein mediate essential functions in murine gammaherpesvirus 68 virion tegumentation and secondary envelopment. *J. Virol.* 86, 1348–1357.
- Wang, S., Wang, K., Li, J., and Zheng, C. (2013). Herpes simplex virus 1 ubiquitin-specific protease UL36 inhibits beta interferon production by deubiquitinating TRAF3. *J. Virol.* 87, 11851–11860.
- Wassermann, R., Gulen, M.F., Sala, C., Perin, S.G., Lou, Y., Rybniker, J., Schmid-Burgk, J.L., Schmidt, T., Hornung, V., Cole, S.T., and Ablasser, A. (2015). *Mycobacterium tuberculosis* differentially activates cGAS- and inflammasome-dependent intracellular immune responses through ESX-1. *Cell Host Microbe* 17, 799–810.
- Watson, R.O., Bell, S.L., MacDuff, D.A., Kimmey, J.M., Diner, E.J., Olivas, J., Vance, R.E., Stallings, C.L., Virgin, H.W., and Cox, J.S. (2015). The cytosolic sensor cGAS detects *Mycobacterium tuberculosis* DNA to induce type I interferons and activate autophagy. *Cell Host Microbe* 17, 811–819.
- Wu, J., Sun, L., Chen, X., Du, F., Shi, H., Chen, C., and Chen, Z.J. (2013). Cyclic GMP-AMP is an endogenous second messenger in innate immune signaling by cytosolic DNA. *Science* 339, 826–830.
- Yang, K., Wang, J., Wu, M., Li, M., Wang, Y., and Huang, X. (2015). Mesenchymal stem cells detect and defend against gammaherpesvirus infection via the cGAS-STING pathway. *Sci. Rep.* 5, 7820.
- Yoneyama, M., Onomoto, K., Jogi, M., Akaboshi, T., and Fujita, T. (2015). Viral RNA detection by RIG-I-like receptors. *Curr. Opin. Immunol.* 32, 48–53.
- Zhang, Z., Yuan, B., Bao, M., Lu, N., Kim, T., and Liu, Y.-J. (2011). The helicase DDX41 senses intracellular DNA mediated by the adaptor STING in dendritic cells. *Nat. Immunol.* 12, 959–965.
- Zhang, X., Wu, J., Du, F., Xu, H., Sun, L., Chen, Z., Brautigam, C.A., Zhang, X., and Chen, Z.J. (2014). The cytosolic DNA sensor cGAS forms an oligomeric complex with DNA and undergoes switch-like conformational changes in the activation loop. *Cell Rep.* 6, 421–430.
- Zhu, F.X., King, S.M., Smith, E.J., Levy, D.E., and Yuan, Y. (2002). A Kaposi's sarcoma-associated herpesviral protein inhibits virus-mediated induction of type I interferon by blocking IRF-7 phosphorylation and nuclear accumulation. *Proc. Natl. Acad. Sci. USA* 99, 5573–5578.
- Zhu, F.X., Chong, J.M., Wu, L., and Yuan, Y. (2005). Virion proteins of Kaposi's sarcoma-associated herpesvirus. *J. Virol.* 79, 800–811.
- Zhu, F.X., Sathish, N., and Yuan, Y. (2010). Antagonism of host antiviral responses by Kaposi's sarcoma-associated herpesvirus tegument protein ORF45. *PLoS ONE* 5, e10573.
- Zinzula, L., and Tramontano, E. (2013). Strategies of highly pathogenic RNA viruses to block dsRNA detection by RIG-I-like receptors: hide, mask, hit. *Antiviral Res.* 100, 615–635.